American Mineralogist, Volume 92, pages 481–490, 2007

Magnetic excitations and heat capacity of fayalite, Fe_2SiO_4

M.C. Aronson,[1] L. Stixrude,[2,*] M.K. Davis,[2] W. Gannon,[1] and K. Ahilan[1]

[1]Department of Physics, University of Michigan, Ann Arbor, Michigan 48109-1120, U.S.A.
[2]Department of Geological Sciences, University of Michigan, Ann Arbor, Michigan 48109-1005, U.S.A.

Abstract

We have used inelastic neutron-scattering measurements to study the magnetic excitations in the antiferromagnetic and paramagnetic phases of polycrystalline fayalite, Fe_2SiO_4. Sharp, nondispersing excitations are found in the ordered state, at 3.3, 5.4, 5.9, and 11.4 meV, and are interpreted as arising from the spin-orbit manifold of the Fe^{2+} ions. These excitations are increasingly damped with increasing temperature, merging into a quasielastic continuum near the 65 K Neel temperature, although their energy does not vary with temperature. We have calculated the contribution of the heat capacity arising from these magnetic excitations and found that it compares favorably with the magnetic heat capacity deduced experimentally. Our analysis indicates that the M1 and M2 sites behave distinctly. The M1 site behaves quasi-locally and appears in the heat capacity as a Schottky anomaly that explains the shoulder in the heat capacity curve near 20 K, while the M2 site contributes predominantly to the critical lambda anomaly. The behavior of fayalite illuminates the nature of magnetic states in several related minerals, including others that also show shoulders and lambda anomalies in the heat capacity (tephroite), those that show only lambda anomalies (cobalt olivine and liebenbergite), and those that show only non-lambda anomalies (bronzite, anthophyllite, and almandine). We find no evidence to support the recent claim that some transition metal silicate and germanate olivines exhibit strong geometric frustration.

Keywords: Fayalite, neutron diffraction, calorimetry, phase transition, magnetic properties

Introduction

Magnetism in minerals is widespread and forms the basis of our knowledge of the past states of the geomagnetic field and plate tectonic motions and deformations of Earth's crust. The foundations of rock magnetism are magnetic ordering and the magnetocrystalline anisotropy: the tendency of moments to align in certain "easy" crystallographic directions below the ordering temperature (O'Reilly 1984). One of the origins of this effect is spin-orbit coupling whereby the local moments respond not only to the mean magnetic field of the other moments or to external fields, but also to their bonding environment via the crystal field (Kittel 1976). The magnetocrystalline anisotropy generally depends strongly on temperature so that re-orientation of the moments is common. The most familiar example in rock magnetism is hematite, which transforms on cooling from a canted to a collinear antiferromagnet at the Morin temperature (265 K) (Morrish 1994). Like the order-disorder transition, canting influences the heat capacity and other thermodynamic properties.

Magnetic and electronic contributions to thermochemical properties can be large (Burns 1993; Wood 1981). The magnetic contribution to the entropy of fayalite is approximately 20% of the total entropy at room temperature (Robie et al. 1982a). The high temperature limiting value for magnetic plus electronic entropy arising from the t_{2g} manifold of an Fe^{2+} ion in an octahedral site is $R\ln 15 = 23$ J/(mol·K), larger than typical entropies of transition among the olivine polymorphs (Akaogi et al. 1989). Since the energy levels and associated thermodynamic contributions are sensitive to crystal structure, magnetic and electronic terms may significantly influence phase stability and element partitioning up to mantle temperatures. Electronic and magnetic excitations are also important for understanding electronic transitions, such as metal-insulator transitions (Williams et al. 1990), and as a probe of atomic scale physics, such as the structure of glasses (Kruger et al. 1992).

While electronic energy levels in minerals have been studied via optical spectroscopy (Burns 1993), comparatively little is known about magnetic energy levels, which are generally taken to be small modifications to the crystal-field levels via spin-orbit coupling. The nature of magnetic excitations can be complex, potentially involving spin waves in magnetically ordered states, spin glass behavior, frustration, critical scattering near the magnetic ordering temperature, and crystal-field excitations at all temperatures. For most minerals, including fayalite, there is no direct spectroscopic information available regarding the modifications to the crystal-field manifold due to magnetic effects; the energies of spin-orbit coupling, and exchange interactions are deduced via non-unique modeling of Mössbauer and magnetic measurements (Ballet et al. 1989; Ehrenberg and Fuess 1993; Fuess et al. 1988). Contributions to this problem from first principles theory are still limited: while spin-orbit coupling and non-collinear magnetism fall within the scope of modern density functional theory, these effects are ignored in recent studies of fayalite (Cococcioni et al. 2003; Jiang and Guo 2004; Wu et al.

* E-mail: stixrude@umich.edu

1996). As electronic structure calculations become both more sophisticated and more ambitious, it is increasingly important that these magnetic degrees of freedom be included, expanding the scope of comparison with experiment (Fang et al. 1998). Thus, it is especially timely to undertake experimental investigations in model systems, carefully chosen to have substantial magnetic character, but also to be geologically relevant.

We have used inelastic neutron-scattering measurements to directly determine the low-lying magnetic excitations in both the paramagnetic and antiferromagnetic states of fayalite (Fig. 1). Fayalite occurs in some meteorites (Hua and Buseck 1995), some highly evolved igneous rocks (Frost et al. 1988), and in high-grade metamorphosed iron formations (Frost 1982), but is geologically most significant as a component of the forsterite-fayalite series that is a common rock forming mineral and the most abundant phase in the upper mantle. The olivine structure has attracted substantial attention recently as exhibiting unusual magnetic properties (Hagemann et al. 2000; Ohgushi and Ueda 2005).

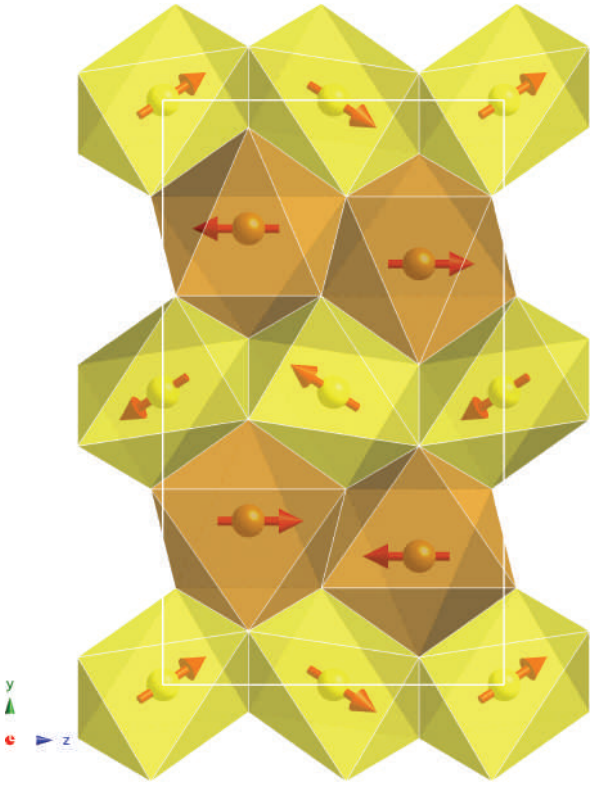

FIGURE 1. Fayalite crystallizes in the orthosilicate olivine structure (*Pbnm*), and the divalent Fe ions occupy two different sites: M1 sites (yellow) with approximate local tetragonal symmetry and M2 sites (brown) with approximate local trigonal symmetry. Fayalite displays a lambda anomaly in the heat capacity and an anomaly in the magnetic susceptibility at the Neel temperature: T_N = 65 K at ambient pressure (Robie et al. 1982a; Santoro et al. 1966) increasing to 100 K at 16 GPa (Hayashi et al. 1987). The magnetic structure is thought to be collinear just below the ordering temperature and to become canted at lower temperature (Lottermoser et al. 1986; Santoro et al. 1966). These elastic neutron-scattering studies find that in the ground state the M2 moments are parallel to [001] (= [010] in the *Pnma* setting), while the M1 moments are canted away from the **c**-axis, and are ferromagnetically coupled. The ground state spin arrangement depicted is consistent with experimental data and theoretical calculations (Cococcioni et al. 2003). The SiO_4 tetrahedra are not shown for clarity.

Unlike optical spectroscopy measurements, inelastic neutron-scattering measurements provide access to the wave vector dependence of excitation energies and linewidths, providing important information about the physical origins and damping of the excitations. Previous inelastic neutron scattering measurements on fayalite have concentrated on the highest energy scales, where the scattering reflects the phonon density of states (Price et al. 1991). By concentrating on smaller neutron energies and smaller wave vectors, our study focuses on the magnetic excitations.

We show how these new measurements help to constrain the magnetic contribution to thermodynamic properties, to unravel electronic from magnetic contributions, and to understand non-lattice contributions even at temperatures well beyond those of our study. In particular, we are able to shed light on three problems that are common to many transition-metal oxides and silicates of geological interest: (1) The persistence of magnetic contributions to thermochemical properties at temperatures well above the Neel temperature (Anovitz et al. 1993; Robie et al. 1982a, 1982b; Stolen et al. 1996). In fayalite, the magnetic entropy is found to be only 80% of the limiting value at the Neel temperature, a deficit that Robie et al. (1982a) attributed to the persistence of local order to higher temperatures. (2) The presence of anomalies in the heat capacity apparently of magnetic origin but not associated with ordering transitions (Krupka et al. 1985; Robie et al. 1982a, 1982b). In fayalite a shoulder appears at 20 K, which has been attributed to a canting transition (Robie et al. 1982a). (3) The relative magnitude and temperature dependence of magnetic, electronic and lattice contributions to thermodynamic properties up to the melting point. Hofmeister (1987) showed that with our limited present knowledge, it is not possible to make quantitative estimates of the magnetic and electronic contributions in fayalite. We also evaluate the recent claim that some transition metal silicate olivines are spin glasses at low temperature (Hagemann et al. 2000).

METHODS

The low-resolution medium-energy chopper spectrometer (LRMECS) at the Intense Pulsed Neutron Source at Argonne National Laboratory was used to measure the inelastic neutron spectra of a 60 g sample of natural polycrystalline fayalite from Crystal Park, Colorado, purchased from Ward Scientific Company (Barker et al. 1975). The sample was examined by optical microscopy, Raman spectroscopy, and powder X-ray diffraction, which yielded peak positions that agreed to within 0.1% with the Powder Diffraction File values. Time of flight spectroscopy is ideal as a survey technique for polycrystalline samples, as it provides simultaneous access to a range of energies and wave vectors for the scattered neutrons, and this range is determined by the incident energy of the neutrons themselves. Incident neutron energies of 10 and 25 meV were used to study the low-lying magnetic excitations, while a limited number of measurements at 50 and 100 meV were used largely to exclude the presence of higher energy magnetic excitations. The data were corrected for the Fe^{2+} form factor, and for self-attenuation, and were placed on an absolute scale by normalization to a vanadium standard. Heat capacity measurements were performed for temperatures from 1.4–100 K using a Quantum Designs Physical Property Measurement System (PPMS) on a 10 mg piece of the neutron scattering sample, using the relaxation method.

RESULTS

We have measured the wave vector q and energy transfer $\Delta E = \hbar\omega$ dependences of the inelastic neutron intensity $S(q,\Delta E)$ of fay-

alite at temperatures from 10–100 K. Contour plots of the scattered intensity with incident neutron energy of 10 meV are presented in Figure 2. Sharp, nondispersing excitations are observed at 10 K, which become less intense and broaden as the temperature is increased. At the same time, a quasielastic background surrounding the elastic peak increases in amplitude with increasing temperature. At temperatures above 55 K, the inelastic peaks have merged with the quasielastic background and are no longer individually resolvable. The quasielastic background develops some structure in the paramagnetic phase (70 K): a pronounced scattering maximum near q~1.3 Å^{-1}, which is the primary (001) wave vector for the antiferromagnetic order in fayalite (Santoro et al. 1966). As the temperature is increased further, to 100 K, the strength of the quasielastic scattering is reduced, and the wave vector dependence becomes less pronounced. This is convincing evidence that the quasielastic scattering is critical scattering, arising from the presence of rapidly fluctuating finite-sized regions in which antiferromagnetic alignment of the moments is present for a finite time interval, and which diverge in size as the temperature approaches T_N from above. To better resolve features at energies nearing that of the incident energy, we repeated the measurements at 10 K with excitations energies of 25 and 50 meV.

The spectrum at 10 K and fixed wavevector (q = 2 ± 0.25 Å^{-1}) highlights the inelastic peaks (Fig. 3). Four excitations are observed at 3.3 meV (peak 1), 5.4 meV (peak 2), 5.9 meV (peak 3), and 11.4 meV (4), superposed on a broad quasielastic background. The two peaks at 5.4 and 5.9 meV overlap considerably and are no longer individually distinguishable at temperatures greater than 20 K.

The inelastic peaks originate from transitions among crystal-field levels of the Fe^{2+} moments on the M1 and M2 sites. We have established this by investigating the variation of peak properties with wavevector. The energies of the four inelastic peaks are remarkably wave vector independent, varying by no more than 2% over our experimental range of q. This observation suggests that the inelastic peaks most likely result from properties of single Fe^{2+} ions, such as crystal-field excitations, and not from spin waves, which would have significant dispersion. The peak intensities decrease with increasing wave vector, as expected from the magnetic form factor. At larger wavevectors, the observed total scattering is enhanced relative to the form factor. The large q behavior is reasonable since we have not attempted to compensate for the phonon contributions to the scattering, which are generally expected to increase approximately quadratically with wave vector (Goremychkin and Osborn 1993; Murani 1983). The influence of nonmagnetic (i.e., phonon) scattering first becomes evident in our data for wave vectors larger than ~3 Å^{-1}.

Although Figure 4 shows that the inelastic peaks can no longer be resolved above the Neel temperature, our data indicate that the underlying energy scales for excitations are largely unmodified.

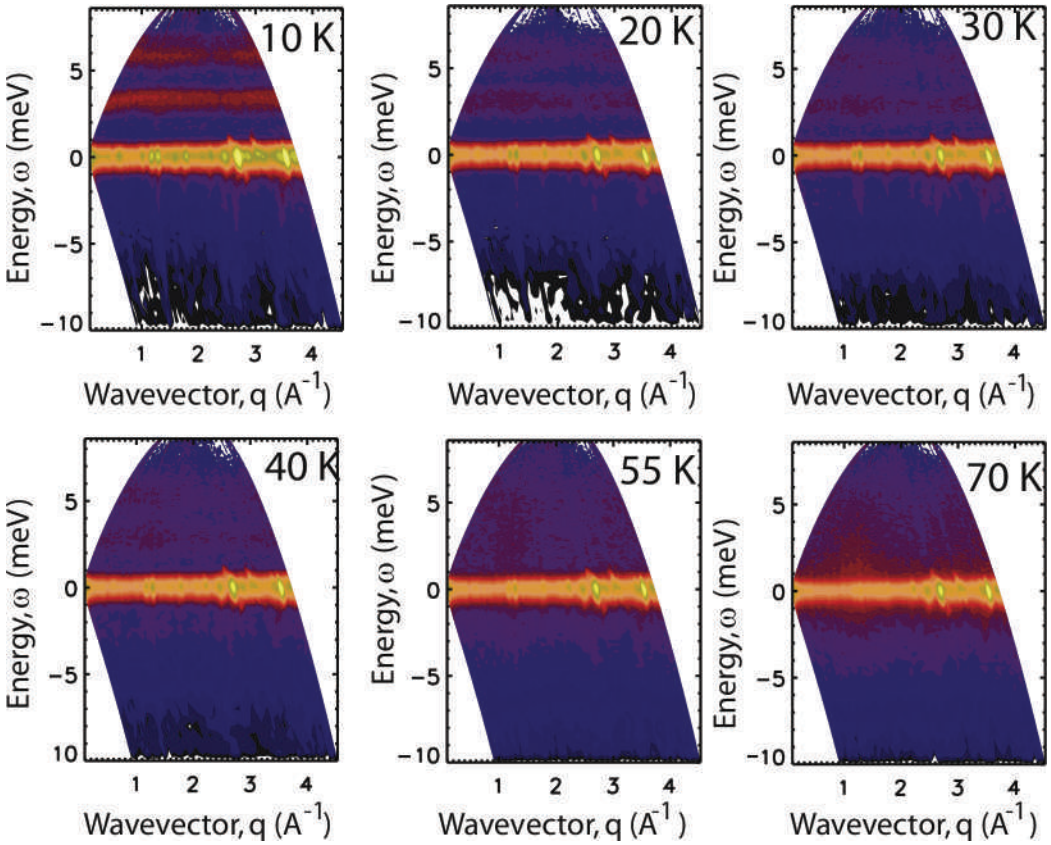

FIGURE 2. Contour plots of the intensity of scattered neutrons S as functions of the wave vector q and neutron energy transfer ω for fayalite at temperatures above and below the 65 K Neel temperature. In each case, the incident neutron energy was 10 meV.

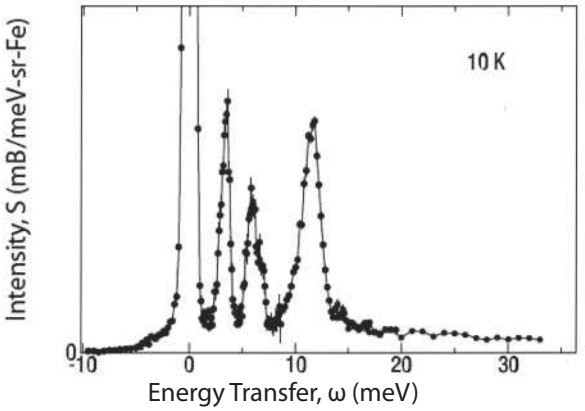

FIGURE 3. The scattered intensity at 10 K, averaged over $q = 2 \pm 0.13$ Å^{-1}, for incident energies of 10, 25, and 50 meV.

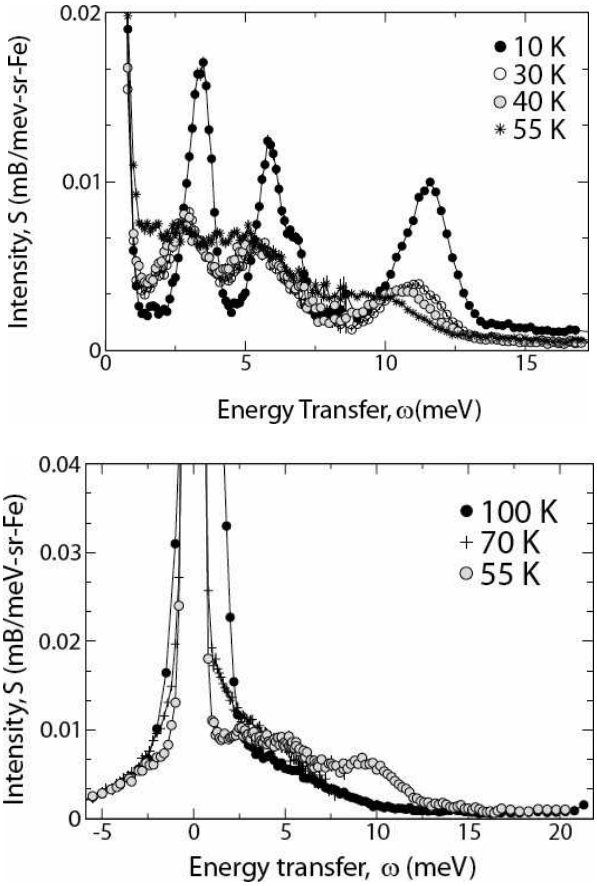

FIGURE 4. Dependence of the scattering on temperature for a fixed wave vector of 2 ± 0.25 Å^{-1}: (**a**) spectra from 10–55 K (**b**) spectra from 55–100 K.

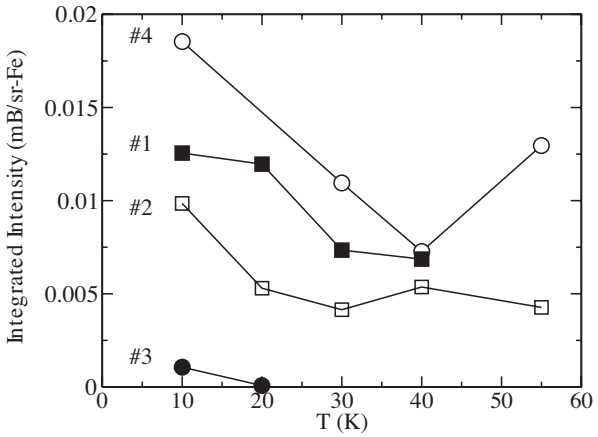

FIGURE 5. Dependence of integrated inelastic peak intensities on temperature at a fixed wavevector of 2 ± 0.25 Å^{-1} as determined from Gaussian fits to the peaks.

As indicated in Figure 5, the intensities of peaks 1, 2, and 4 initially decrease rapidly with increased temperature, but approach temperature-independent values above 40 K. The inelastic peak energies decrease modestly as the temperature approaches the Neel temperature. Interestingly, the percentage decrease in energy between 10 and 40 K is almost the same for each peak: 25% for Peak 1, 23% for Peak 2, and 19% for Peak 4. In each case, the inelastic energies remain large as the system approaches antiferromagnetic order. Thus, there is no suggestion that the underlying excitations vanish with the onset of antiferromagnetic order at 65 K, which might be expected if the related energy levels result from exchange splitting of the crystal-field manifold, absent in the paramagnetic state. Instead, we believe that the lifetimes of these excitations are dramatically suppressed by critical scattering near T_N, and that they are subsequently absorbed into the increasing quasielastic background with increased temperature.

We have measured the heat capacity of a 10 mg piece of polycrystalline fayalite, taken from the larger neutron scattering sample (Fig. 6). The data agree well with the previous report (Robie et al. 1982a). To estimate the phonon contribution to the heat capacity, we measured the heat capacity of polycrystalline monticellite, $CaMgSiO_4$. The monticellite heat capacity is rescaled according to the scheme of (Robie et al. 1982b), which reproduces well the high temperature γ-Ca_2SiO_4 results (King 1957) that were previously used to verify the magnetic entropy of Fe_2SiO_4 (Robie et al. 1982a). We have independently estimated the phonon contribution following the preferred model (D-ND), based on zone-center vibrational spectra of Hofmeister (1987). The phonon contributions estimated in these two ways differ by about 1 J/(mol·K) at 100 K.

Subtraction of the phonon contribution reveals a magnetic heat capacity for fayalite that decreases continuously above the Neel temperature, implying a substantial contribution from critical fluctuations (Fig. 6). It is apparent from this comparison that the magnetic component of the total heat capacity is larger than the nonmagnetic component at all temperatures below the Neel temperature, and is about a quarter of the total heat capacity at 100 K.

ANALYSIS

Magnetic excitations

Our observations that the energies of the inelastic peak do not change with wave vector, and that the wave vector dependence of the peak intensity is well described by the Fe^{2+} form factor

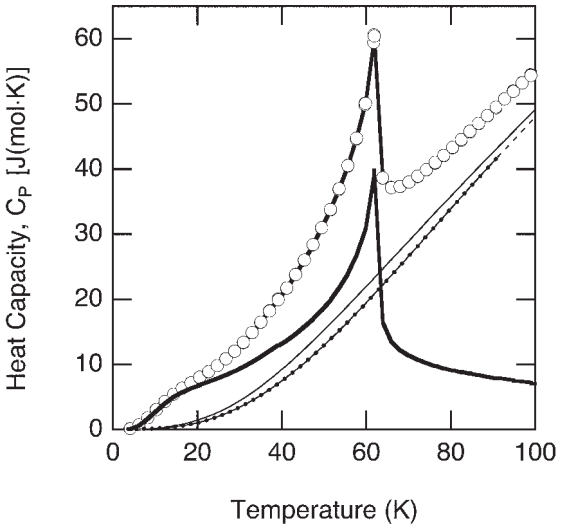

FIGURE 6. The measured heat capacity of fayalite (open circles) and monticellite (filled circles). The temperatures of the monticellite data have been rescaled by 11% to reproduce the high-temperature heat capacity of γ-Ca_2SiO_4 (King 1957), a nonmagnetic reference (Robie et al. 1982a, 1982b). The thin solid line is an alternative estimate of the lattice heat capacity from the vibrational density of states model D-ND of Hofmeister (1987). The thick solid line indicates the magnetic heat capacity of fayalite, obtained by subtracting the scaled monticellite heat capacity data from the total fayalite heat capacity.

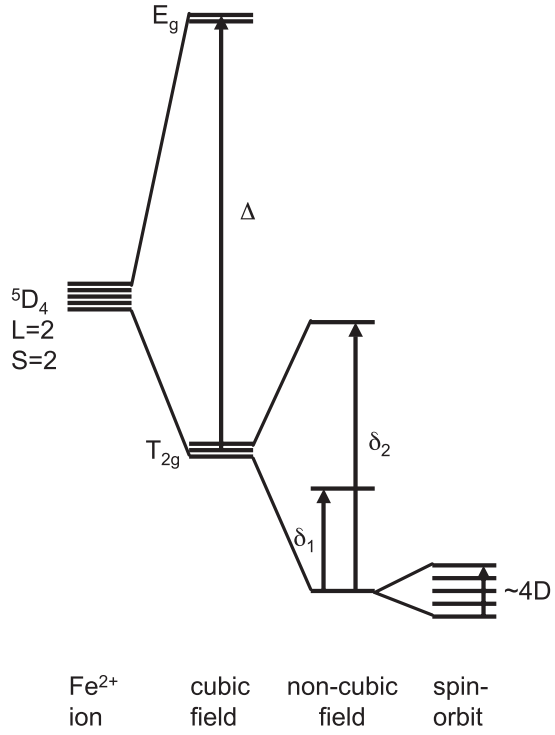

FIGURE 7. The subsequent effects of a cubic crystal field, a non-cubic field, and the spin orbit coupling on the states of the Fe^{2+} ion.

are strong arguments that all four of the inelastic peaks result from excitations among discrete levels in the crystal-field split manifold of Fe^{2+} atomic states (Fig. 7). To interpret our data, we consider a scheme that has been widely used to understand the properties of fayalite and other Fe-bearing silicates (Ballet and Coey 1982; Burns 1970, 1985; Coey et al. 1981; Ehrenberg and Fuess 1993; Runciman et al. 1973). In free space, Fe^{2+} has the configuration $3d^6$, $^5D_4$, and is 25-fold degenerate. The crystal field is primarily octahedral and splits the manifold into a low lying T_{2g} triplet, and an E_g doublet. The magnitude of the splitting is sufficiently large (~9000 cm^{-1}), that we may safely ignore the E_g doublet in our analysis. The T_{2g} manifold is further split due to lowered site symmetry at M1 (approximately tetragonal D_{4h}) and M2 (approximately trigonal C_{3v}) sites, producing excitations from the groundstate within the T_{2g} manifold δ_1 and δ_2. Spin-orbit coupling further splits the ground state. In a trigonal field, the width of the spin-orbit manifold is 4D with $D \approx \lambda^2/\delta_1$ (Varret and Hartmann-Boutron 1968), where the spin-orbit coupling parameter for the free ion is $\lambda \approx 100$ cm^{-1} (Figgis 1966). We assume that the details of the ground-state splittings within this sub-manifold are different for the M1 and M2 sites, not only because the relative strength and symmetry of the axial fields are different, but also because the exchange splitting depends on the details of the moment coupling and geometry.

We assume that inelastic peaks at 3.3, 5.4, 5.9, and 11.4 meV arise from spin-orbit excitations. This assignment is consistent with previous work: the width of the spin-orbit manifold is of order 10 meV in other Fe-bearing silicates (Coey et al. 1981), while the next lowest excitation beyond the spin-orbit manifold, δ_1, is expected to lie at higher energy than the range of our measurements (Burns 1985). For general symmetry, we would expect eight spin-orbit excitations, four each for the M1 and M2 sites, distinguished by their distinct crystal fields (Carlin and van Duyneveldt 1977). Realistically, we would not expect to resolve all peaks as smaller splittings would only be partially resolved, for example, the difference between the 5.4 and 5.9 meV peaks.

Magnetic heat capacity

This crystal field scheme can be tested experimentally, by comparison to the temperature dependence of the heat capacity. The low temperature heat capacity ($T < 20$ K) can be quantitatively explained by a Schottky anomaly arising from the spin-orbit excitations (Fig. 8). The Schottky contribution is computed as the temperature derivative of the magnetic energy E_S

$$E_S = \frac{\sum_{i=1}^{n} g_i \varepsilon_i \exp\left(-\varepsilon_i / kT\right)}{\sum_{i=1}^{n} g_i \exp\left(-\varepsilon_i / kT\right)} \quad (1)$$

where g_i and ε_i are the degeneracy and energy of level i, k is the Boltzmann constant, T is the temperature, and we have neglected the temperature dependence of the level energies. We find agreement with the heat capacity data if we assume that the total number of levels $\Sigma g_i = 5$, so that only one of the two distinct Fe sites contributes to the Schottky anomaly. We suggest that this is the M1 site, for reasons discussed below, and that the M2

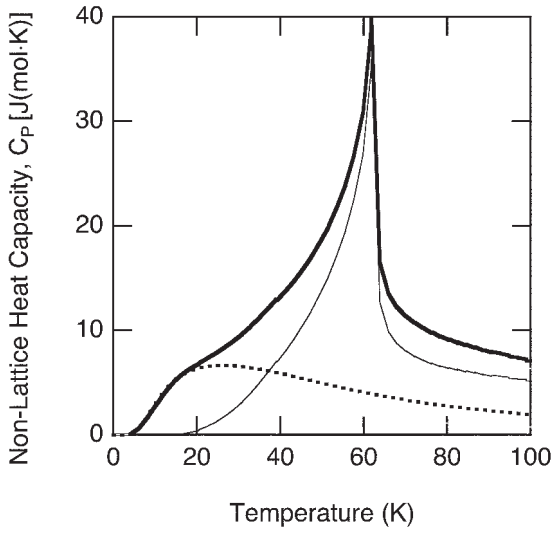

FIGURE 8. The non-lattice heat capacity of fayalite (bold line) compared with the computed Schottky contribution (dashed line) and the difference (light solid line).

TABLE 1. Energy levels in fayalite

Energy, meV (cm^{-1})	Assignment	Degeneracy	Site	Ref.
0	ground state	1	M1	This work
3.3 (27)	spin-orbit	1	M1	This work
5.9 (47)	spin-orbit	1	M1	This work
11.4 (92)	spin-orbit	2	M1	This work
91 (730)	δ_1	5	M1	Burns (1985)
186 (1500)	δ_2	5	M1	Burns (1985)
0	ground state	1	M2	This work
<1 (8)	spin-orbit	3	M2	This work
5.4 (44)	spin-orbit	1	M2	This work
207 (1670)	$\delta_1 + \delta_2$	10	M2	Burns (1985)

site is largely responsible for the lambda anomaly at T_N. The set of levels and degeneracies for the M1 site specified in Table 1 reproduce the low-temperature heat capacity to within experimental precision. The calculated heat capacity is very sensitive to the assumed degeneracy of the two lowest lying excitations; if either of these is made doubly degenerate, or if we include the 5.4 meV as well as the 5.9 meV as singlets in this analysis, the low-temperature heat capacity is overestimated by 1.5–2.5 J/(mol·K). If the ground state is made doubly degenerate, the heat capacity is underestimated by 3 J/(mol·K). We conclude that the 5.4 and 5.9 meV peaks represent two distinct excitations, and that they must arise from two distinct iron sites. As expected, the calculation in the vicinity of the 20 K heat capacity anomaly is not sensitive to the degeneracy of the highest lying excitation at 11.4 meV. We stress that there are no adjustable parameters in the calculation of the Schottky heat capacity, and that the level spacings are known independently from the neutron scattering measurements on the same sample.

There has been much controversy about the origin of the 20 K heat capacity shoulder. A neutron diffraction study (Santoro et al. 1966) first proposed the possibility of a spin canting transition on the M1 site, although a subsequent study (Fuess et al. 1988) with more comprehensive temperature coverage found no evidence for such a transition. Nonetheless, an analysis of the magnetization and its anisotropy (Ehrenberg and Fuess 1993) indicated a change in the spin canting direction on M1 below ~20 K, a finding which was consistent with temperature dependent hyperfine fields, taken from several Mössbauer experiments (Hafner et al. 1990; Lottermoser et al. 1995, 1996). Our experiments suggest a very different scenario. Specifically, we suggest that the shoulder in the heat capacity near 20 K results from the thermal population of the lowest lying excited states in the crystal-field-split manifold of the M1 site, lying 3.3 meV, and 5.9 meV above a singlet ground state. It is possible that the temperature dependent occupancies of excited states with different symmetries may also be responsible for the temperature dependences of the hyperfine fields, and their anisotropy. A conclusive identification of the symmetry properties of these states is still lacking, and would be required to make quantitative comparison to the Mössbauer results.

Computation of the Schottky contribution isolates a second part of the magnetic heat capacity, which is sharply peaked at the Neel temperature, while vanishing both above and below (Fig. 8). The form of this contribution suggests that it originates with antiferromagnetic critical fluctuations, which contribute a power-law divergence to the temperature dependent heat capacity, centered at the phase transition, as we observe. As discussed further below, we associate the critical anomaly with the M2 site. We have assigned the remaining peak (2 at 5.4 meV) to the M2 site (Table 1). The other spin-orbit excitations on this site are not resolved by our measurements; we have assigned them small values as discussed further below. The thermal population of the spin-orbit manifold on the M2 site is governed by the exchange interaction; the local picture inherent in Equation 1 does not apply and the contribution of the M2 site to the heat capacity is a lambda, rather than a Schottky, anomaly.

The limiting value of the magnetic entropy is not reached in fayalite until about twice the Neel temperature (Fig. 9). Analysis of the magnetic entropy reveals the origin of this behavior. Computation of the limiting value assumes that the spin-orbit manifold is fully occupied, so that there are $2S + 1 = 5$ equally occupied states. In fact, the temperature evolution of the Schottky contribution to the magnetic entropy shows that the spin-orbit manifold is not fully occupied until about twice the Neel temperature in the case of fayalite. The limiting value of the magnetic entropy cannot then be achieved at temperatures less than $2T_N$ regardless of the state of magnetic order. At the Neel temperature, the Schottky contribution to the magnetic entropy is $1.34R \approx R\ln(3.8)$. Simply put, the development of magnetic order in fayalite involves not only the conventional growth of magnetic correlations with reducing temperature (Robie et al. 1982a), but the simultaneous reduction of the effective moment due to freezing out of the highest lying levels of the spin-orbit manifold.

Further support for the notion that incomplete occupation of the spin-orbit manifold, rather than magnetic order account for much of the temperature evolution of the magnetic entropy above T_N comes from comparison with other materials (Fig. 10). In the case of the itinerant moment ferromagnet Ni, crystal field effects are absent. The magnetic entropy reaches its limiting value at the ordering temperature and does not increase further at higher temperatures. The case of Ni confirms the conventional view that the entire magnetic entropy is removed

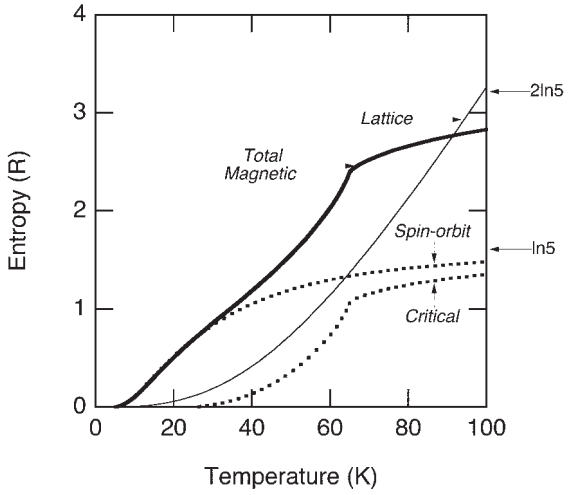

FIGURE 9. Contributions to the entropy in fayalite as indicated compared with the ideal high-temperature values expected of the magnetic contribution per site.

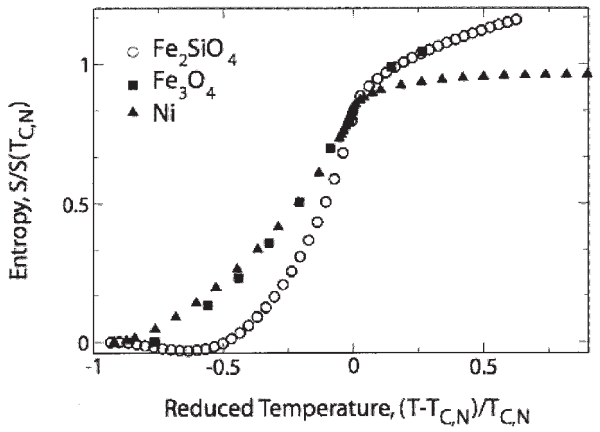

FIGURE 10. The evolution of the magnetic entropy in fayalite (this work), magnetite (Gronvold and Sveen 1974), and nickel (Meschter et al. 1981) with the temperature scaled to the magnetic ordering temperature ($T_{C,N}$), and the entropy scaled to the value at the ordering temperature.

with magnetic ordering. On the other hand, another material (magnetite) with a spin-orbit manifold of finite width shows a temperature dependence of the magnetic entropy above T_N that is very similar to what we find in fayalite, suggesting that like fayalite, the effective moment degeneracy is still evolving, due to spin-orbit or crystal field splittings with energies comparable to the ordering temperature itself.

Magnetic and electronic heat capacity

The non-lattice heat capacity at higher temperatures shows distinctive behavior that probes energy levels beyond the spin-orbit manifold (Fig. 11). The non-lattice heat capacity decreases with increasing temperature until a well-defined minimum near 170 K and then increases with increasing temperature again. This behavior reflects the saturation of the spin-orbit manifold while the

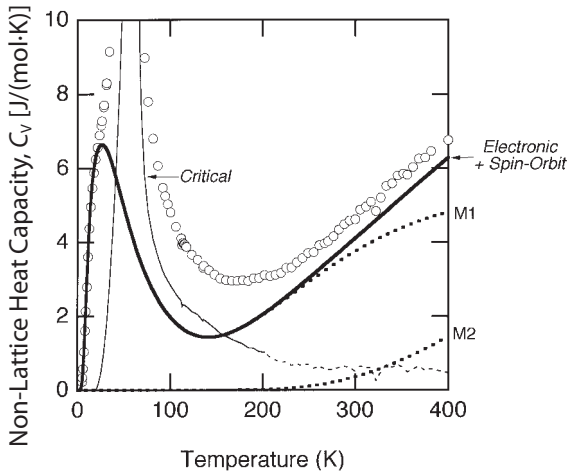

FIGURE 11. The non-lattice heat capacity of fayalite (circles) compared with the computed contributions from the M1 and M2 sites (dashed) and their sum (bold solid line) considering magnetic and electronic contributions. The remainder (light solid line) is the critical contribution and is shown dashed when its value falls below nominal uncertainties in the phonon contribution [1 J/(mol·K)].

crystal-field levels δ_1 and δ_2 become increasingly populated.

The gradual transition from magnetic to electronic dominated non-lattice heat capacity can be quantitatively explained by our results in combination with previous investigations of the crystal-field excitations (Table 1). The complete series of levels for the M1 site (neglecting only the E_g states) are defined by our measurements of the spin-orbit levels and values for δ_1 and δ_2 on this site from Burns (1985). We have concluded that the M2 site is dominated by critical fluctuations at low temperature (see further discussion below), and so its contribution to the magnetic heat capacity is not amenable to a simple treatment. To compute the contribution of the M2 site to the electronic heat capacity, we have included a fivefold degenerate ground state, together with the values of δ_1 and δ_2 for this site from Burns (1985).

The computed non-lattice heat capacity agrees well with the experimentally estimated value from the highest temperatures of the measurements of Robie et al. (1982a) down to a temperature of about 200 K where critical fluctuations start to become important (Fig. 11). The experimental value of the non-lattice contribution to the isochoric heat capacity C_V is estimated by subtracting from the measured values of C_P the phonon contribution and the correction from C_P to C_V according to C_P-C_V = 4.9 mJ/mol $K^{-2}T$ (Hofmeister 1987). The difference between computed and experimental non-lattice heat capacity is less than 0.5 J/(mol·K), well within the uncertainty of the lattice correction in the range 250–400 K. The deviation of the computed and experimental curves at temperatures 20–250 K is due to the un-modeled critical fluctuation contribution from the M2 site. The contribution from critical fluctuations, obtained by subtracting the modeled heat capacity from the measured non-lattice contribution, decreases with increasing temperature and falls below the uncertainty in the phonon contribution [~1 J/(mol·K)] at a temperature of 200 K. Our result for the critical contribution disagrees with the proposal that partial magnetic order persists to temperatures greater than

500 K, based on an analysis of Raman line broadening (Kolesov and Geiger 2004).

Discussion

Our results suggest that the M1 and M2 sites make separable and complementary contributions to the heat capacity. On the M1 site, the spin-orbit manifold is thermally populated as if the Fe ion were isolated, providing a sequence of Schottky-like contributions to the heat capacity both above and below T_N, but no clear contribution to the lambda anomaly at T_N. The absence of conventional long-range magnetic order on the M1 sites is upheld by neutron diffraction measurements, which find a linear increase of the M1 staggered moment for $T < T_N$, previously ascribed to weak Fe-Fe coupling (Ehrenberg and Fuess 1993). This explanation agrees with a first-order understanding of superexchange (Cox 1992): this is weakest when the Fe-O-Fe angle between neighboring octahedra is 90°, as is the case of M1-M1 neighbors, and greatest as the angle increases: the angle is 130° for M2-M2 neighbors. Not only is the exchange interaction more important for the M2 site, the width of the spin-orbit manifold is inferred to be smaller. In our proposed scheme (Table 1), the width of the spin-orbit manifold on M2 is a factor of two smaller than that on M1. More complete quenching on M2 is consistent with the value of δ_1 on this site being approximately twice that on M1 according to the assignment of Burns (1985). Since the exchange interaction is much more important than spin-orbit, the M2 site provides no Schottky contribution and contributes only to the lambda anomaly. In agreement, the order parameter determined from neutron diffraction measurements (Ehrenberg and Fuess 1993) indicates that the staggered moment on the M2 site displays a near mean-field like temperature dependence, vanishing smoothly at T_N.

The case of kirschsteinite lends additional insight into the unique nature of the M1 sites, which resists conventional magnetic order to the lowest temperature. In this phase, Fe^{2+} occupies only the M1 sites. It shows no magnetic ordering down to at least 4 K (Newnham et al. 1966). This is additional evidence that, as in fayalite, intersite interactions on the M1 sites are weak and that the relevant physics on this site is largely local.

Studies of pressure-amorphized fayalite also point to different magnetic behavior of the two cation sites (Kruger et al. 1992). Whereas in the crystalline phase both M1 and M2 sites order at the Neel temperature, in the amorphous material, one site orders at 65 K and the other at 28 K. The authors argued that geometric frustration lowers the ordering temperature on one class of sites while leaving the other class of sites unaffected. Our analysis suggests an alternative interpretation, that the lower ordering temperature corresponds to M1-like sites and that the lowering is primarily due to weak M1-M1 exchange interactions.

The case of fayalite illuminates the magnetic properties of other transition-metal olivines. Tephroite, cobalt olivine, and liebenbergite all show Neel temperatures within a factor of two of that of fayalite. However, only tephroite also shows a shoulder in the heat capacity. We suggest that the shoulder in tephroite has the same origin as that in fayalite: thermal population of the spin-orbit manifold on the M1 site. This suggestion is consistent with the very similar temperature dependence of the magnetic structure in fayalite and tephroite (Santoro et al. 1966). The shoulder in tephroite occurs at a slightly lower temperature than that in fayalite. This result can be understood in terms of a narrower spin-orbit manifold in tephroite caused by the smaller spin-orbit coupling parameter of the Mn^{2+} ion ($\lambda \sim 60$ cm^{-1}) as compared with that of Fe^{2+} ($\lambda \sim 100$ cm^{-1}) (Figgis 1966). Our explanation of the heat capacity of tephroite disagrees with Robie et al. (1982b) who argued for a magnon contribution to the heat capacity on the basis of the form of the temperature dependence. As we have argued here, an acceptable account of the temperature dependence of the heat capacity is possible in fayalite considering only spin-orbit excitations and critical scattering, without requiring an appreciable magnon contribution, which in any case is ruled out by our inelastic scattering data. We suggest that a similar explanation may well be appropriate for the heat capacity in tephroite, although inelastic neutron scattering experiments would be required to definitively prove that this is the case.

The ions Co^{2+} and Ni^{2+} have much larger spin-orbit coupling parameters ($\lambda \sim 170$ and 630 cm^{-1}, respectively) (Figgis 1966). These values are sufficiently large that essentially no thermal excitation within the spin-orbit manifold occurs in cobalt olivine up to the Neel temperature. Indeed, the magnetic heat capacity saturates at a value $2R\ln 2$, corresponding to a reduced value of the effective spin $S = 1/2$, as opposed to the value $S = 3/2$ that one would expect based on Hund's rules (Robie et al. 1982b).

Recently it has been suggested that magnetic order is suppressed in some transition metal silicate and germanate olivines through frustration effects intrinsic to the olivine lattice via triangular elements of the arrangement of transition metal ions (Hagemann et al. 2000). The degree of frustration is reflected in the ratio $f = \theta_{CW}/T_N$ of the Curie-Weiss constant to the Neel temperature: values $f > 10$ are thought to correspond to strong geometric frustration, where the ordering transitions are suppressed to unusually low temperatures, given relatively strong spin-spin interactions, and where the persistence of short range order severely broadens the phase transition region (Ramirez 1994). Our data and previous results cited in the Table 2, although not those of Hagemann et al. (2000), reveal several difficulties with this argument. First, the basic magnetic parameters measured by Hagemann et al. disagree severely in some cases with previous results. Literature values indicate much smaller values of f. Second, the heat capacity of silicate olivines with one type of transition metal cation all show a prominent and sharp lambda anomaly at a temperature that agrees well with the Neel temperature as determined from magnetic susceptibility measurements. Finally, elastic neutron diffraction demonstrates an ordered spin arrangement in tephroite below T_N (Santoro et al. 1966). We believe that available data rule out the possibility of strong geometric frustration in tephroite, cobalt olivine, leibengerbite, fayalite, or Mn-germanate olivine. Instead, we suggest that θ_{CW} in the olivines cannot be considered a reliable measure of the spin-spin interactions, but more generally is modified in the presence of the low-lying spin-orbit excitations that lead to a temperature-dependent moment.

We anticipate that Schottky-like anomalies should appear in other Fe^{2+}-bearing minerals, since the spin-orbit manifold should be grossly similar to that in fayalite. The Schottky anomaly should be revealed most clearly in those systems with weak spin-

TABLE 2. Transition metal silicate and germanate olivines

Mineral name	Formula	T_2 (K)	T_N (K)	θ_{CW} (K)	f	Ref.
–	$CaCoSiO_4$	–	16	1	0.1	Newnham et al. (1966)
Kirschsteinite	$CaFeSiO_4$	–	<4	12	–	Newnham et al. (1966)
Glaucochroite	$CaMnSiO_4$	–	9	26	2.9	Caron et al. (1965)
–	Co_2SiO_4	–	49	65	1.3	Nomura et al. (1964)
		–	48	55	1.1	Kondo and Miyahara (1966)
		–	49	46	0.9	Hagemann et al. (2000)
		–	50	–	–	Robie et al. (1982b)
Fayalite	Fe_2SiO_4	20	65	150	2.3	Santoro et al. (1966)
		23	62	165	2.7	Kondo and Miyahara (1966)
		16	65			Robie et al. (1982a)
		20	65			This work
–	Mn_2GeO_4	–	24	162	6.8	Creer and Troup (1970)
		–	14	166	11.9	Hagemann et al. (2000)
Tephroite	Mn_2SiO_4	12	50	163	3.3	Santoro et al. (1966)
		15	75	175	2.3	Kondo and Miyahara (1966)
		–	14	171	12.2	Hagemann et al. (2000)
		12	47	–	–	Robie et al. (1982b)
Liebenbergite	Ni_2SiO_4	–	30	7	0.2	Newnham et al. (1965)
		–	33	15	0.5	Kondo and Miyahara (1966)
		–	32	35	1.1	Hagemann et al. (2000)
		–	29	–	–	Robie et al. (1984)

Note: T_2 refers to the temperature of a second anomaly in the magnetic susceptibility other than the Neel temperature or to a shoulder in the heat capacity other than the lambda anomaly.

TABLE 3. Other Fe^{2+} bearing minerals

Mineral name	Formula	X_{Fe}	T_2 (K)	T_N (K)	Ref.
Bronzite	$(Mg_{1-x}Fe_x)_2Si_2O_6$	0.15	13	<5	Krupka et al. (1985)
Anthophyllite	$(Mg_{1-x}Fe_x)_7Si_8O_{22}(OH)_2$	0.1	13	<5	Krupka et al. (1985)
Diopside	$CaMgSi_2O_6$	0.01	10	<5	Krupka et al. (1985)

Note: X_{Fe} is the fraction of divalent cation sites occupied by Fe atoms.

spin interactions. Indeed, there are several dilute Fe^{2+} minerals that do display Schottky-like anomalies in the heat capacity (Table 3). The temperature and width of these anomalies are similar to that in fayalite. Almandine is an unusual case because the shoulder in the heat capacity noted by Anovitz et al. (1993) may also be due to an anomalous temperature dependence in the lattice heat capacity, due to the mismatch in size between the Fe^{2+} ion and the large dodecahedral site, as also found in pyrope. In the case of bronzite, the low-temperature heat capacity has been modeled as a Schottky anomaly (Krupka et al. 1985) but without a physical picture and with parameters fit to the heat capacity data, rather than derived by independent means as we have done. We suggest that the anomalies in these materials arise from the Fe^{2+} spin-orbit manifold, a prediction that could be tested via inelastic neutron-scattering experiments.

ACKNOWLEDGMENTS

We acknowledge stimulating discussions with P. de Chatel and E. Essene, and the technical assistance of Alexander Kolesnikov during the neutron-scattering experiments, and R. Rouse for the X-ray diffraction analysis. We are especially grateful to W. Montfrooij for generously providing software for the analysis of time of flight neutron scattering data. Work at the University of Michigan was performed under the auspices of the U.S. Department of Energy under grant DE-FG02-94ER45526 (Physics) and the National Science Foundation under grant EAR-0230154 (Geological Sciences).

REFERENCES CITED

Akaogi, M., Ito, E., and Navrotsky, A. (1989) Olivine-modified spinel-spinel transitions in the system Mg_2SiO_4-Fe_2SiO_4—Calorimetric measurements, thermochemical calculation, and geophysical application. Journal of Geophysical Research—Solid Earth and Planets, 94, 15671–15685.

Anovitz, L.M., Essene, E.J., Metz, G.W., Bohlen, S.R., Westrum, E.F., and Hemingway, B.S. (1993) Heat-capacity and phase-equilibria of almandine, $Fe_3Al_2Si_3O_{12}$. Geochimica et Cosmochimica Acta, 57, 4191–4204.

Ballet, O. and Coey, J.M.D. (1982) Magnetic-properties of sheet silicates—2-1 layer minerals. Physics and Chemistry of Minerals, 8, 218–229.

Ballet, O., Fuess, H., Wacker, K., Untersteller, E., Treutmann, W., Hellner, E., and Hosoya, S. (1989) Magnetization measurements of the synthetic olivine single-crystals Mn_2SiO_4, Fe_2SiO_4 or Co_2SiO_4. Journal Of Physics—Condensed Matter, 1, 4955–4970.

Barker, F., Wones, D.R., Sharp, W.N., and Desborough, G.A. (1975) Pikes peak batholith, colorado front range, and a model for the origin of the gabbro-Anorthosite-Syenite-Potassic Granite Suite. Precambrian Research, 2, 97–160.

Burns, R.G. (1970) Crystal field spectra and evidence of cation ordering in olivine minerals. American Mineralogist, 55, 1608–1632.

——— (1985) Thermodynamic data from crystal-field spectra. In S.W. Kieffer and A. Navrotsky, Eds., Microscopic To Macroscopic: Atomic Environments to Mineral Thermodynamics, 14, p. 277–315. Reviews in Mineralogy, Mineralogical Society of America, Chantilly, Virgina.

——— (1993) Mineralogical Applications of Crystal Field Theory. Cambridge University Press, U.K.

Carlin, R.L. and van Duyneveldt, A.J. (1977) Magnetic Properties of Transition Metal Compounds. Springer-Verlag, New York.

Caron, L.G., Santoro, R.P., and Newnham, R.E. (1965) Magnetic structure of $CaMnSiO_4$. Journal of Physics and Chemistry of Solids, 26, 927–930.

Cococcioni, M., Dal Corso, A., and de Gironcoli, S. (2003) Structural, electronic, and magnetic properties of Fe_2SiO_4 fayalite: Comparison of LDA and GGA results. Physical Review B, 67, 094106.

Coey, J.M.D., Ballet, O., Moukarika, A., and Soubeyroux, J.L. (1981) Magnetic-properties of sheet silicates—1-1 layer minerals. Physics and Chemistry of Minerals, 7, 141–148.

Cox, P.A. (1992) The Transition Metal Oxides. Oxford University Press, U.K.

Creer, J.G. and Troup, G.J.F. (1970) Crystal and magnetic structures of Mn_2GeO_4. Solid State Communications, 8, 1183–1188.

Ehrenberg, H. and Fuess, H. (1993) Analytical interpretation and simulation of the static magnetic-properties of synthetic alpha-Fe_2SiO_4. Journal of Physics—Condensed Matter, 5, 3663–3672.

Fang, Z., Terakura, K., Sawada, H., Miyazaki, T., and Solovyev, I. (1998) Inverse versus normal NiAs structures as high pressure phases of FeO and MnO. Physical Review Letters, 81, 1027–1030.

Figgis, B.N. (1966) Introduction to Ligand Fields. Interscience Publishers, New York.

Frost, B.R. (1982) Contact metamorphic effects of the Stillwater Complex, Montana—the concordant iron-formation—a discussion of the role of buffering in metamorphism of iron-formation. American Mineralogist, 67, 142–148.

Frost, B.R., Lindsley, D.H., and Andersen, D.J. (1988) Fe-Ti oxide-silicate equilibria—assemblages with fayalitic olivine. American Mineralogist, 73, 727–740.

Fuess, H., Ballet, O., and Lottermoser, W. (1988). Magnetic phase transition in olivines M_2SiO_4 (M = Mn, Fe, Co, Fe_xMn_{1-x}). In S. Ghose, and J.M.D. Coey, Eds. Advances in Physical Geochemistry, 7, p. 185–207. Springer Verlag, New York.

Goremychkin, E.A. and Osborn, R. (1993) Crystal-field excitations in $CeCu_2Si_2$. Physical Review B, 47, 14280–14290.

Gronvold, F. and Sveen, A. (1974) Heat-capacity and thermodynamic properties of synthetic magnetite (Fe_3O_4) from 300 to 1050 K—ferrimagnetic transition and zero-point entropy. Journal Of Chemical Thermodynamics, 6, 859–872.

Hafner, S.S., Stanek, J., and Stanek, M. (1990) Fe-57 Hyperfine interactions in the magnetic phase of fayalite, Fe_2SiO_4. Journal of Physics and Chemistry of Solids, 51, 203–208.

Hagemann, I.S., Khalifah, P.G., Ramirez, A.P., and Cava, R.J. (2000) Geometric magnetic frustration in olivines. Physical Review B, 62, R771–R774.

Hayashi, M., Tamura, I., Shimomura, O., Sawamoto, H., and Kawamura, H. (1987) Antiferromagnetic transition of fayalite under high-pressure studied by Mössbauer-spectroscopy. Physics and Chemistry of Minerals, 14, 341–344.

Hofmeister, A.M. (1987) Single-crystal absorption and reflection infrared-spectroscopy of forsterite and fayalite. Physics and Chemistry of Minerals, 14, 499–513.

Hua, X. and Buseck, P.R. (1995) Fayalite in the kaba and mokoia carbonaceous chondrites. Geochimica et Cosmochimica Acta, 59, 563–578.

Jiang, X.F. and Guo, G.Y. (2004) Electronic structure, magnetism, and optical properties of Fe_2SiO_4 fayalite at ambient and high pressures: A GGA+U study. Physical Review B, 69, 155108.

King, E.G. (1957) Low temperature heat capacities and entropies at 298.15 K of some crystalline silicates containing calcium. Journal of the American Chemical Society, 79, 5437–5438.

Kittel, C. (1976) Introduction to solid state physics. Wiley, New York.

Kolesov, B.A. and Geiger, C.A. (2004) A temperature-dependent single-crystal Raman spectroscopic study of fayalite: evidence for phonon-magnetic excitation coupling. Physics and Chemistry of Minerals, 31, 155–161.

Kondo, H. and Miyahara, S. (1966) Magnetic properties of several orthosilicates with olivine structure. Journal of the Physical Society of Japan, 21, 2193–2196.

Kruger, M.B., Jeanloz, R., Pasternak, M.P., Taylor, R.D., Snyder, B.S., Stacy,

A.M., and Bohlen, S.R. (1992) Antiferromagnetism in pressure-amorphized Fe_2SiO_4. Science, 255, 703–705.
Krupka, K.M., Robie, R.A., Hemingway, B.S., Kerrick, D.M., and Ito, J. (1985) Low-temperature heat-capacities and derived thermodynamic properties of anthophyllite, diopside, enstatite, bronzite, and wollastonite. American Mineralogist, 70, 249–260.
Lottermoser, W., Forcher, K., Amthauer, G., and Fuess, H. (1995) Powder-crystal and single-crystal Mössbauer-spectroscopy on synthetic fayalite. Physics and Chemistry of Minerals, 22, 259–267.
Lottermoser, W., Muller, R., and Fuess, H. (1986) Antiferromagnetism in synthetic olivines. Journal of Magnetism and Magnetic Materials, 54-7, 1005–1006.
Lottermoser, W., Forcher, K., Amthauer, G., Treutmann, W., and Hosoya, S. (1996) Single crystal Mössbauer spectroscopy on the three principal sections of a synthetic fayalite sample in the antiferromagnetic state. Physics and Chemistry of Minerals, 23, 432–438.
Meschter, P.J., Wright, J.W., Brooks, C.R., and Kollie, T.G. (1981) Physical contributions to the heat-capacity of nickel. Journal of Physics and Chemistry of Solids, 42, 861–871.
Morrish, A.H. (1994) Canted Antiferromagnetism: Hematite. World Scientific, Singapore.
Murani, A.P. (1983) magnetic spectral response in the intermetallic compound $CeSn_3$. Physical Review B, 28(4), 2308–2311.
Newnham, R., Santoro, R., Fang, J., and Nomura, S. (1965) Antiferromagnetism in nickel orthosilicate. Acta Crystallographica, 19, 147–148.
Newnham, R.E., Caron, L.G., and Santoro, R.P. (1966) Magnetic properties of $CaCoSiO_4$ and $CaFeSiO_4$. Journal of the American Ceramic Society, 49, 284–285.
Nomura, S., Newnham, R., Fang, J., and Santoro, R. (1964) Antiferromagnetism in cobalt orthosilicate. Journal of Physics and Chemistry of Solids, 25, 901–905.
Ohgushi, K. and Ueda, Y. (2005) Anomalous magnetic properties near the spin-flop bicritical point in Mn_2AS_4 (A = Si and Ge). Physical Review Letters, 95, 217202.
O'Reilly, W. (1984) Rock and Mineral Magnetism. Chapman and Hall, New York.
Price, D.L., Ghose, S., Choudhury, N., Chaplot, S.L., and Rao, K.R. (1991) Phonon density of states in fayalite, Fe_2SiO_4. Physica B, 174, 87–90.
Ramirez, A.P. (1994) Strongly Geometrically Frustrated Magnets. Annual Review of Materials Science, 24, 453–480.
Robie, R.A., Finch, C.B., and Hemingway, B.S. (1982a) Heat capacity and entropy of fayalite (Fe_2SiO_4) between 5.1 and 383 K: comparison of calorimetric and equilibrium values for the QFM buffer reaction. American Mineralogist, 67, 463–469.
Robie, R.A., Hemingway, B.S., and Takei, H. (1982b) Heat capacities and entropies of Mg_2SiO_4, Mn_2SiO_4, and Co_2SiO_4 between 5 and 380 K. American Mineralogist, 67, 470–482.
Robie, R.A., Hemingway, B.S., Ito, J., and Krupka, K.M. (1984) Heat capacity and entropy of Ni_2SiO_4 olivine from 5 to 1000 K and heat capacity of Co_2SiO_4 from 360 to 1000 K. American Mineralogist, 69, 1096–1101.
Runciman, W.A., Sengupta, D., and Gourley, J.T. (1973) Polarized spectra of iron in silicates. 2. Olivine. American Mineralogist, 58, 451–456.
Santoro, R.P., Newnham, R.E., and Nomura, S. (1966) Magnetic Properties of Mn_2SiO_4 and Fe_2SiO_4. Journal of Physics and Chemistry of Solids, 27, 655–666.
Stolen, S., Glockner, R., Gronvold, F., Atake, T., and Izumisawa, S. (1996) Heat capacity and thermodynamic properties of nearly stoichiometric wustite from 13 to 450 K. American Mineralogist, 81, 973–981.
Varret, F. and Hartmann-Boutron, F. (1968) Effects of spin-orbital coupling on properties of ionic magnetic compounds of iron group at low transition temperature. Annales De Physique, 3, 157–168.
Williams, Q., Knittle, E., Reichlin, R., Martin, S., and Jeanloz, R. (1990) Structural and electronic-properties of Fe_2SiO_4-fayalite at ultrahigh pressures—amorphization and gap closure. Journal of Geophysical Research—Solid Earth and Planets, 95, 21549–21563.
Wood, B.J. (1981) Crystal field electronic effects on the thermodynamic properties of Fe^{2+} minerals. In R.C. Newton, A. Navrotsky, and B.J. Wood, Eds., Thermodynamics of minerals and melts, p. 63–84. Springer-Verlag, New York.
Wu, Z., Mottana, A., Marcelli, A., Natoli, C.R., and Paris, E. (1996) Theoretical analysis of X-ray absorption near-edge structure in forsterite, Mg_2SiO_4-*Pbnm*, and fayalite, Fe_2SiO_4-*Pbnm*, at room temperature and extreme conditions. Physics and Chemistry of Minerals, 23, 193–204.

Manuscript received May 9, 2006
Manuscript accepted November 16, 2006
Manuscript handled by George Lager